Novel Binderless Granulated Molecular Sieves for Thermochemical Heat Storage

Jochen Jänchen[1*], Alfons Brandt[2], Jens Schmeißer[2], Baldur Unger[2], Helmut Stach[3] and Udo Hellwig[1]

[1]Technical University of Applied Sciences Wildau, Bahnhofstraße, 15745 Wildau, Germany

[2]Chemiewerk Bad Köstritz GmbH, Heinrichshall 2, 07586 Bad Köstritz, Germany.

[3]ZeoSolar e.V., Volmerstraße 13, 12489 Berlin-Adlershof, Germany.

* Corresponding Author, j.e.jaenchen@t-online.de

Abstract

The thermochemical storage properties and water adsorption of novel binderless molecular sieves have been investigated by thermogravimetry, hydrothermal stability tests, water isotherm measurements and tests in a closed lab-scaled thermochemical storage. The new zeolites 13XBF and 4ABF show improved storage densities, higher performances, higher discharging temperatures and hydrothermal stability comparable with conventional granulated zeolites of the same structure type.

1. Introduction

Zeolites roused up the interest in application of energy savings through energy storage and to solar energy by developing a "green" energy supply. These strategies are based on thermochemical storage by adapted zeolites with special properties such as high specific storage capacity for long-term storage materials or fast ad- and desorption processes for heat driven heat pumps [1-4]. To improve the molecular sieve properties in terms of those energetic application demands we developed novel binderless materials and tested them by a comparative study. This study focuses on the hydrothermal stability, the water adsorption properties, and the thermochemical storage behaviour.

2. Experimental

Two new binderless KÖSTROLITH® products, 4ABF and 13XBF, as well as the commonly used KÖSTROLITH® 13XK and a low-silica X, NaLSX, have been chosen in this study to investigate their morphology, hydrothermal stability, water adsorption properties, and storage behaviour. The new products (13XBF and 4ABF) have been prepared following a novel strategy of manufacturing to get stable binderless beads of improved adsorption capacity.

The morphology has been checked by a JEOL JSM640 scanning electron microscope (SEM) combined with energy dispersive X-ray analysis (EDX).

The hydrothermal tests have been performed in a programmable oven (Ströhlein) with a reactor tube of about 2 L volume. The reactor tube is connected to a 1-L-flask with approximately 0.5 L saturated $MgCl_2$ solution serving as vaporizer or condenser with a constant relative humidity of 33%. A

membrane vacuum pump, a pressure sensor (Balzers) and a data acquisition system complete the setup of the apparatus. A thermocouple for registration of the sample temperature is located between oven wall and the reactor tube and a second one for the vaporizer/condenser temperature is placed outside of the flask close to the surface of the salt solution.

The water adsorption properties have been examined by thermogravimetry (TG) on a Setaram TG-DSC 111 equipment with heating rates of 3 K/min to a temperature of 723 K (nitrogen stream 1 L/h) starting with samples saturated at water p/p_s=0.33. Furthermore, the adsorption behaviour has been measured by adsorption isotherms at 293 and 353 K using a McBain balance.

Lab-scaled tests with about 1 kg of zeolite have been performed in a thermochemical storage of 1.5 L volume to evaluate the storage properties such as energy storage density and maximum temperature in the storage (for more information cf. [1]). Additionally, tests on a larger scale have been performed in a 35-L-storage connected to a 12 m^2 vacuum tube collector array for solar charging of the storage material. In this case the charging temperature was limited to 385 K (for more information cf. [5]).

3. Modelling

The results of our isotherm measurements were extrapolated using the well known Dubinin-approach to obtain isosteres from the measured isotherm data in an extended temperature (273-573 K) and pressure (0.001-1000 mbar) range. The characteristic curves of the adsorption systems and other relevant dependences such as isotherms, isobars, and isosteres can be calculated using the Dubinin theory of pore filling [6]. The Dubinin approach considers the pore volume as crucial (in contrast to the inner surface of the micropores) because the adsorbed molecules (comparable in size with the micropores) are influenced by overlapping adsorption potentials generating large heats of adsorption. Dubinin defines the specific volume, W, of the adsorption space (cavities and pores in cm^3 of the microporous material in g) as:

$$W = a/\rho_{ads} , \qquad\qquad\qquad (1)$$

where a = adsorbed amount in g/g, depending on T and p, and ρ_{ads} = density of the adsorbate in g/cm^3, depending on T, and the differential work of adsorption, A, is defined as:

$$A = -\Delta f = RT (\ln p_s/p) , \qquad\qquad\qquad (2)$$

where Δf = free energy and p_s = vapour pressure of the adsorptive in equilibrium with the liquid bulk phase at the analysis temperature, T. Dubinin found for many adsorption systems with activated carbon that almost all experimental systems have a single curve relating W and A. The relation W = f(A) is called the "characteristic curve" which is temperature invariant for many adsorption systems and well applicable to the system water/zeolite (for further details see Stach et al. [7]).

4. Results and discussion

Fig. 1 shows the SEM images of the bead surfaces of 13XBF and 4ABF, respectively. Both technical products are well crystallized molecular sieves exhibiting no binder which covers the zeolite crystal surfaces. A binder often disturbs the mass transfer. Because of a missing binder an improved mass transfer is expected for this type of molecular sieves.
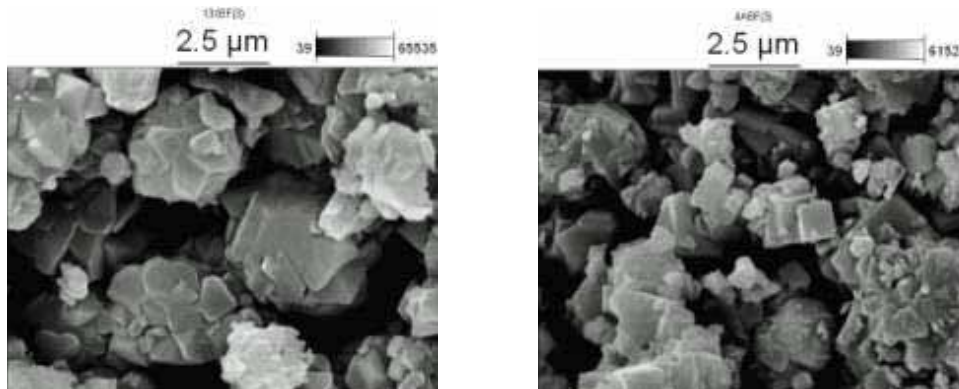
Fig. 1. SEM images of the surface of 13XBF-beads 1.6-2.5 mm (left hand side) and 4ABF-beads (right hand side).
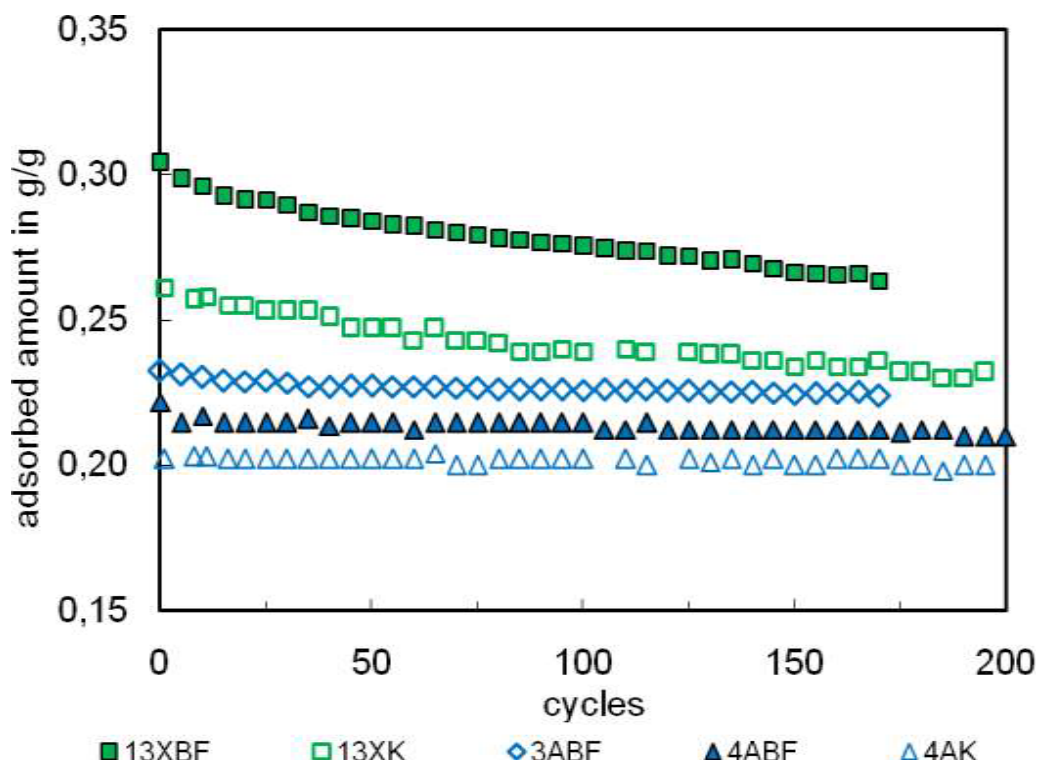

Fig. 2. Hydrothermal stability tests of 13XBF and 4ABF compared to the ordinary types X and A with binder, conditions: T=295K-620K, 10-15 mbar H_2O.

Fig. 2 compares the changes of the water adsorption capability of the molecular sieves upon a cyclic hydrothermal treatment. For this test about 5 g of water saturated zeolite (of known dry weight) have been put into the reactor tube. The reactor tube with the samples and the vessel containing the salt solution were carefully degassed followed by starting the temperature program to desorb the samples.

The desorption procedure follows heating with 20 K/min from room temperature up to 350 °C, dwelling at 350 °C for another 44 min and cooling down to room temperature over night. At the next morning the heating program was started again. After 5 cycles the water adsorption capacity was checked as an indication for the degree of degradation of the crystallinity.

As can be seen from Fig. 2 a significant difference in the hydrothermal stability of X- and A-type zeolites is found. The 4ABF and 4AK materials practically do not change their adsorption capacity upon the hydrothermal treatment. 13XBF and 13XK show a degradation of their adsorption capacities, however, under harsher conditions as would be likely in the thermochemical storage. Finally, no difference in the hydrothermal stability between the ordinary molecular sieves and the binderless materials of types 13X and 4A could be identified under the chosen conditions.

The results of the TG experiments show, as expected, improved adsorption capacities for the binderless samples. The 13XBF adsorbs 0.32 g/g, about 10% more water compared to ordinary 13XK (0.29 g/g) and NaLSX (0.28 g/g) because of the missing binder. Even the binderless WE894 (a former product from Bayer, a=0.26 g/g) reveals a significant lower adsorption capacity proving an exceptional value for the water adsorption capacity of 13XBF as a technical product. The molecular sieve 4ABF has a lower capacity (for structural reasons) but with a=0.25 g/g a rather high value as well.
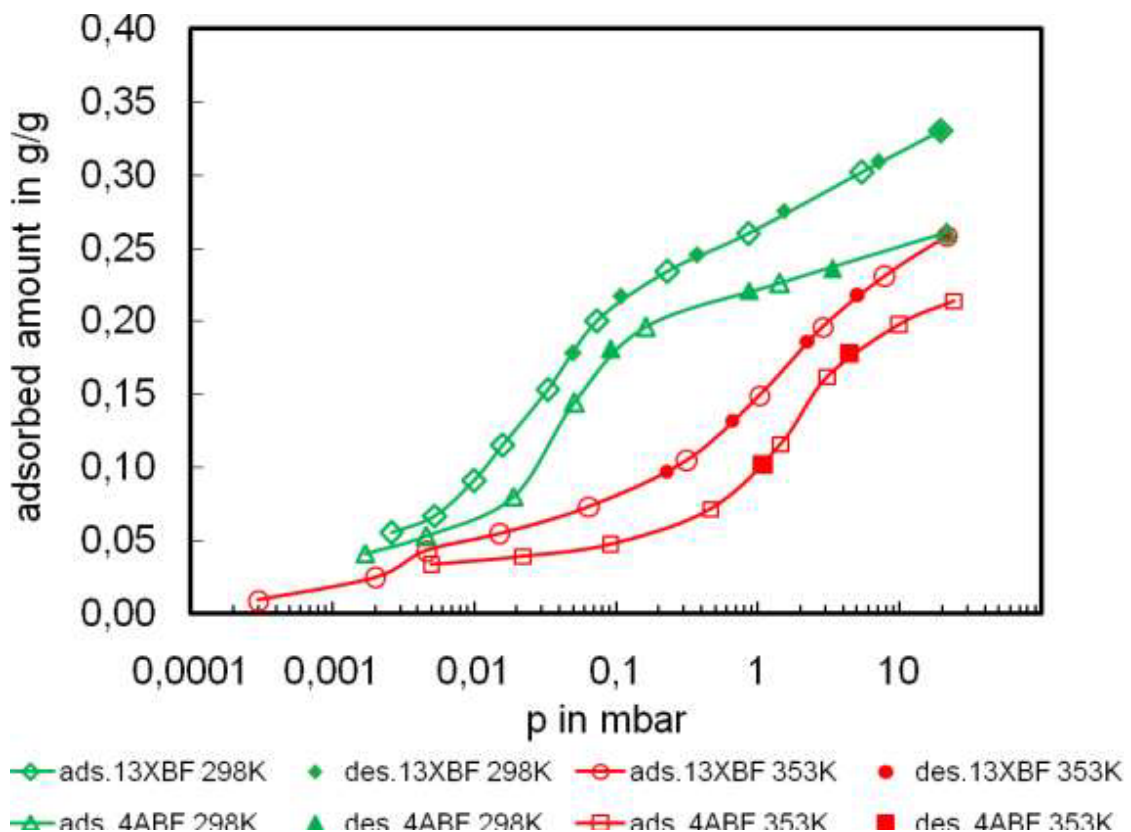

Fig. 3. Water adsorption isotherms of 13XBF and 4ABF at T=298 and 353 K, filled symbols denote desorption.
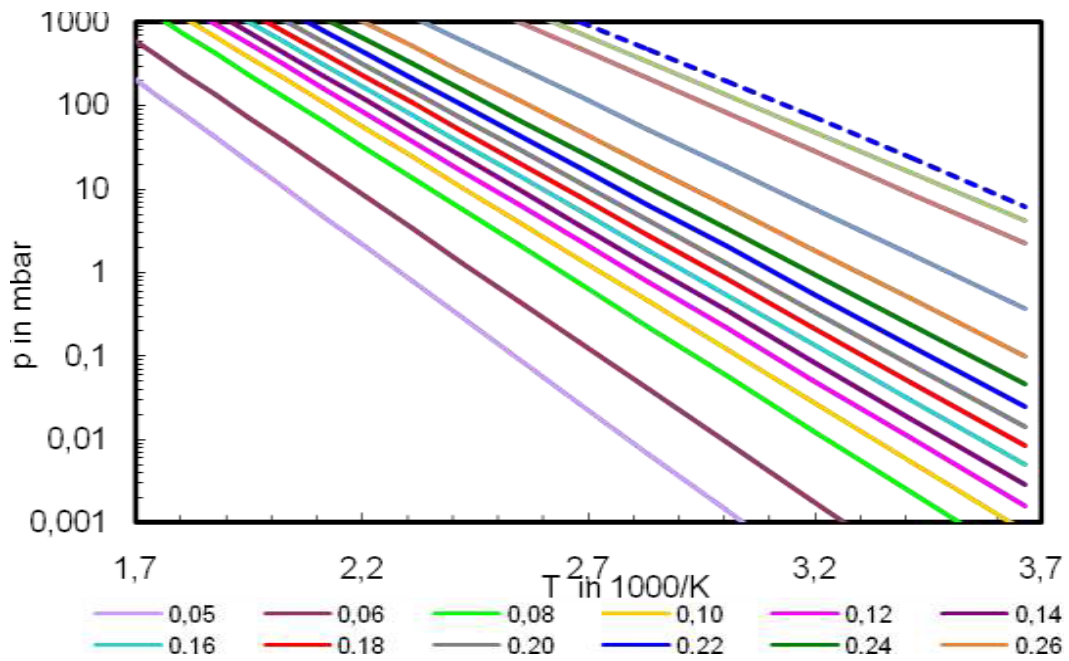
Fig. 4. Adsorption isosteres of water for 13XBF, calculated from the isotherms using the Dubinin equation, parameter of the isosteres: a in g/g, dotted line corresponds to the vaporization/condensation of water.
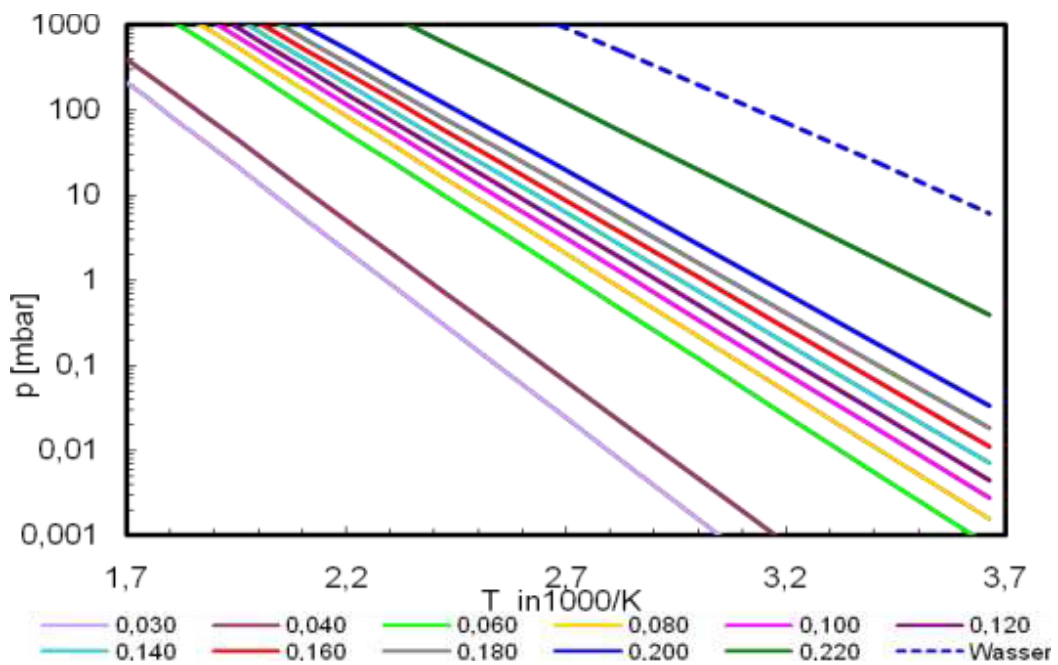

Fig. 5. Adsorption isosteres of water for 4ABF, calculated from the isotherms using the Dubinin equation, parameter of the isosteres: a in g/g, dotted line corresponds to the vaporization/condensation of water.

Fig. 3 summarizes the results of the isotherm measurements for 13XBF and 4ABF. Typical s-shaped reversible isotherms have been found which can be modelled by applying the Dubinin equation [6]. A fast equilibration was obvious after dosing of a certain amount of water vapour indicating faster kinetics compared with the binder containing samples. As described previously by calculation of the temperature invariant characteristic curve other relevant thermodynamic data can be determined. Fig. 4 and 5 give an example of the adsorption isosteres for 13XBF and 4ABF. Those diagrams are important input data to describe the storage cycle consisting of charging and discharging at certain given T and p conditions.

The isotherm measurements already pointed to fast equilibration of the water in the binderless molecular sieves. This observation explains a significantly higher performance of the storage material during discharging (adsorption of water) represented by higher temperatures in the storage (13XBF, 4ABF, cf. Tab. 1).
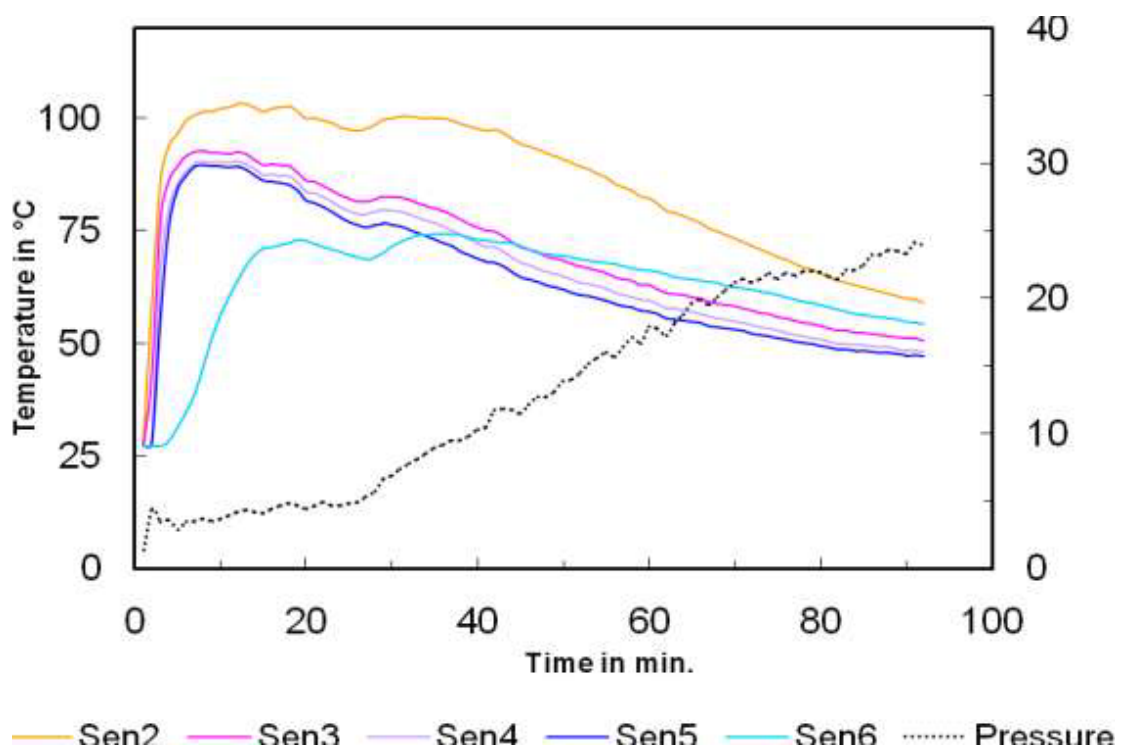

Fig. 6. Example of temperatures (left hand side axis) in the storage material at different storage positions and the water vapour pressure in mbar (right hand side).

Table 1. Results of the tests in the lab-scaled storage (1.5 L) for 13X molecular sieves and 4ABF

Sample	Desorption temperature in K	Adsorbed amount a, in kg/kg	T_{max} (storage) in K	Energy density in Wh/kg
4ABF	470	0.180	393	131
13XBF	470	0.220	378	166
13XK	470	0.200	370	156
NaLSX	470	0.243	370	159
NaLSX (solar)*	385	0.150	264	130

* determined in a 35-L-storage connected to a vacuum tube collector array

Furthermore, Tab. 1 shows an improved adsorption capacity and storage density for 13XBF compared to the other 13X zeolites. Interestingly, because of the unusual fast kinetics of the BF-materials the vaporizer of our storage (for the water vapour supply) came sometimes to its limit.

Fig. 6 gives an example of the temperature profiles during discharging of 13XBF in the storage. Sensor 6 shows lower temperatures because of insufficient water vapour supply at that position in the storage.

NaLSX (Tab.1) gives an example of the reduced storage capacity by charging in a solar driven 35-L-storage at a limited temperature. It is expected to get a better result for 13XBF. Faster kinetics of desorption of the BF-zeolites might contribute to a less reduced storage capacity by solar charging of the storage because the given time limit of the daily solar radiance beside the limited temperature is compensated by the faster kinetics. The measurements are in progress.

5. Conclusion

The binderless novel molecular sieves are well suited for thermochemical storage but also for drying and heat transformation applications and probably for solar applications due to fast kinetics, high water adsorption capacity, sufficient hydrothermal stability and improved storage capacity.

6. Acknowledgement

References

[1] J. Jänchen, D. Ackermann, H. Stach, W. Brösicke, Solar Energy **76** (2004) 339.

[2] J. Jänchen, D. Ackermann, E. Weiler, H. Stach, W. Brösicke, Thermochimica Acta **434** (2005) 37.

[3] J. Bauer, R. Herrmann, W. Mittelbach, W. Schwieger, Int. J. Energy Research **33** (2009) 1233.

[4] J. Jänchen, D. Ackermann and H. Stach; in: R.Z.Wang, Z.Lu, W. Wang and X. Huang (Ed.) Proceedings of the International Sorption Heat Pump Conference (ISHPC) 2002, 24-27 September 2002, Shanghai, PR China, Science Press New York Ltd.,2002, p. 635-638.

[5] J. Jänchen, D. Ackermann, E. Weiler, H. Stach, W. Brösicke, Proceedings of the Third Workshop of IEA/ECES, Annex 17, 1-2 October 2002, Tokyo, Japan, www. fskab.com/Annex17/

[6] M.M. Dubinin, Bull Division of Chem. Soc. (1960) pp.1072-1078.

[7] H. Stach, J. Mugele, J. Jänchen, E. Weiler, Adsorption **11** (2005) 393.